

# Quadrotor prototype

Jorge Miguel Brito Domingues

Instituto Superior Técnico

Portugal, October 2009

**Abstract** - There is currently a limited diversity of vehicles capable of Vertical Take-Off and Landing. However there is a visible interest by scholars and admirers of Unmanned Aerial Vehicles for a particular type of aircraft called quadrotor. This work aims precisely at the design and control of a quadrotor prototype having a tri-axis accelerometer and a compass as its sensors.

This project started with the design of the quadrotor having in mind a list of objectives to be fulfilled by it. Then followed the modeling of the dynamics and kinematics of the aircraft's motion, as well as of its motors and sensors. This led to the implementation of the quadrotor in a computer simulation environment called Simulink®.

Given the outputs provided by the available sensors, a Kalman filter was developed capable of estimating the angular velocities and Euler angles of the quadrotor, being therefore possible to have knowledge of its attitude. This filter was combined with a Linear-Quadratic Regulator in order to make the system follow a given attitude reference. Finally, the results of the simulations and real implementation in the quadrotor are presented.

**Keywords** - Quadrotor modeling, quadrotor simulation, Kalman filter, Linear-Quadratic Regulator.

## I. INTRODUCTION

A quadrotor, or quadrotor helicopter, is an aircraft that becomes airborne due to the lift force provided by four rotors usually mounted in cross configuration, hence its name. It is an entirely different vehicle when compared with a helicopter, mainly due to the way both are controlled. Helicopters are able to change the angle of attack while the blades are in rotation, quadrotors cannot.

At present, there are two main areas of quadrotor development: transportation (of goods and people) and Unmanned Aerial Vehicles (UAVs) [1]. UAVs can be classified into two major groups: heavier-than air and lighter-than-air. These two groups self divide in many other that classify aircrafts according to motorization, type of liftoff and many other parameters. Vertical Take-Off and Landing (VTOL) UAVs like quadrotors have several advantages over fixed-wing airplanes. They can move in any direction in its lateral plane and are capable of hovering and fly at low speeds. In addition, the VTOL capability allows deployment in almost any terrain while fixed-wing aircraft require a prepared airstrip for takeoff and landing. Given these characteristics, quadrotors can be used in search and rescue missions, meteorology, penetration of hazardous

environments (e.g. exploration of other planets) and other applications suited for such an aircraft. Also, they are playing an important role in research areas like control engineering, where they serve as prototypes for real life applications.

## II. QUADROTOR OPERATION

Each rotor in a quadrotor is responsible for a certain amount of thrust and torque about its center of rotation, as well as for a drag force opposite to the rotorcraft's direction of flight. The quadrotor's propellers are not all alike. In fact, they are divided in two pairs, two pusher and two puller blades, that work in contra-rotation. As a consequence, the resulting net torque can be null if all propellers turn with the same angular velocity, thus allowing for the aircraft to remain still around its center of gravity.

In order to define an aircraft's orientation (or attitude) around its center of mass, aerospace engineers usually define three dynamic parameters, the angles of yaw, pitch and roll. This is very useful because the rotational forces used to control the aircraft act around its center of mass, causing it to pitch, roll or yaw. Pitch rotation is induced by contrary variation of speeds in propellers 1 and 3 (see Fig. 1), resulting in forward or backwards translation. If we do this same action for propellers 2 and 4, we can produce a change in the roll angle and we will get lateral translation. Yaw is induced by mismatching the balance in aerodynamic torques (i.e. by offsetting the cumulative thrust between the counter-rotating blade pairs). So, by changing these three angles in a quadrotor we are able to make it maneuver in any direction (Fig. 2).

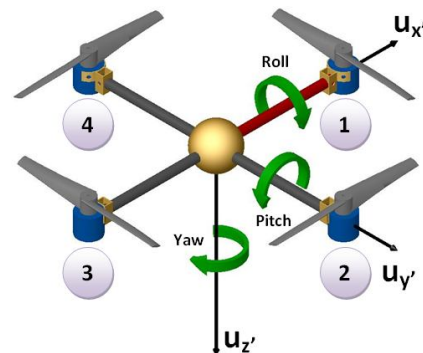


Fig. 1. Yaw, pitch and roll rotations of a common quadrotor.

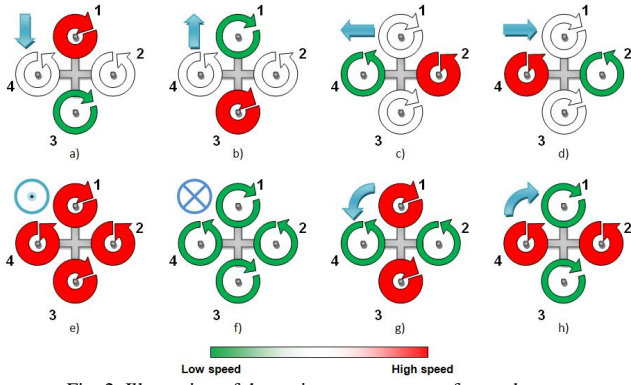


Fig. 2. Illustration of the various movements of a quadrotor.

### III. QUADROTOR DESIGN

#### A. General concept

Designing an aircraft is a demanding and crucial stage that can bring us significant advantages in the future, such as avoiding unnecessary delays in the aircraft's assembly stage. In this section we will define our mission to build a quadrotor prototype suitable for indoor flight, as well justify the decisions and equipment chosen for achieving this purpose. At this point it is therefore relevant to define the main goals in the general design:

- Overall mass not superior to 1 kg. When it comes to quadrotors, the heavier they get, the more expensive they are. Many quadrotors used for research do not exceed this mass. So, aiming for a maximum mass of 1 kg seems to be a suitable target;
- Flight time between 10 and 20 minutes. There is no point in using the quadrotor for 2 minutes and then wait a couple of hours to recharge the batteries, wasting precious time;
- On-board controller should have its separate power supply to prevent simultaneous engine and processor failure in case of battery loss;
- Ability to transmit live telemetry data and receive movement orders from a ground station wirelessly, therefore avoiding the use of cables which could become entangled in the aircraft and cause an accident;
- The quadrotor should not fly very far from ground station so there is no need of long range telemetry hardware and the extra power requirements associated with long range transmissions.

Consequently, the main components should be:

- 4 electric motors and 4 respective Electronic Speed Controllers (ESC);
- 4 propellers with 0.254 m in diameter;
- 1 on-board processing unit;
- 1 tri-axis analog accelerometer. Measuring acceleration in three-dimensional space aboard an aircraft is a necessary feat to understand the magnitude of the forces acting on this aircraft. It may also be possible to use this sensor to calculate the angles of yaw and pitch with knowledge of the gravity acceleration vector;
- 1 electronic compass to measure the yaw angle;
- 2 on-board power supplies (batteries), one for the motors and another to the processing unit. At this point we will

assume that beyond the need to provide electrical power to the motors, we must assure that the brain of the quadrotor (i.e. the on-board processing unit) remains working well after the battery of the motors has discharged;

- 1 airframe for supporting all the aircraft's components.

#### B. Propellers

The typical behavior of a propeller can be defined by three parameters [2]: the thrust coefficient  $c_T$ , power coefficient  $c_P$  and propeller radius  $r$ . These parameters allow the calculation of a propeller's thrust  $T$ :

$$T = c_T \frac{4\rho r^4}{\pi^2} \omega^2 \quad (1)$$

and power  $P_p$ :

$$P_p = c_P \frac{4\rho r^5}{\pi^3} \omega^3 \quad (2)$$

where  $\omega$  is the propeller angular speed and  $\rho$  the density of air. These formulas show that both thrust and power increase greatly with propeller's diameter. If the diameter is big enough, then it should be possible to get sufficient thrust while demanding low rotational speed of the propeller. Consequently, the motor driving the propeller will have lower power consumption, giving the quadrotor higher flight time. The calculated power and thrust coefficients for the chosen propeller are:

$$c_P = 0.1154 \quad (3)$$

$$c_T = 0.0743 \quad (4)$$

In reality, neither the thrust nor the power coefficients are constant values, they are both functions of the advance ratio  $J$  [3]:

$$J = \frac{u_0}{nD_p} \quad (4)$$

where  $u_0$  is the aircraft flight velocity,  $n$  is the propeller's speed in revolutions per second, and finally  $D_p$  is the propeller diameter.

However, when observing the characteristic curves for both these coefficients (see [3]), it is clear that when an aircraft's flight velocity is low, their values remain constant, which is the current case, for at this point there is only interest in achieving a hovered flight, with no interest in achieving high translation velocity (note that accelerometers provide bad estimates of the gravity vector, and therefore attitude, when subject to other external forces). The curves in Fig. 3 show the thrust and propeller power as a function of propeller angular speed (using (1) and (2)). Knowing that the final weight of the quadrotor is 0.820 kg, we can see from Fig. 3 that these propellers, together, are well capable of providing

the 8.04 N necessary for Take-Off. An illustration of the quadrotor prototype is presented in Fig. Y. The quadrotor uses an Arduino electronics prototyping platform the width of a PWM (Pulse-Width Modulation) signal to control the angular speed of the motors.

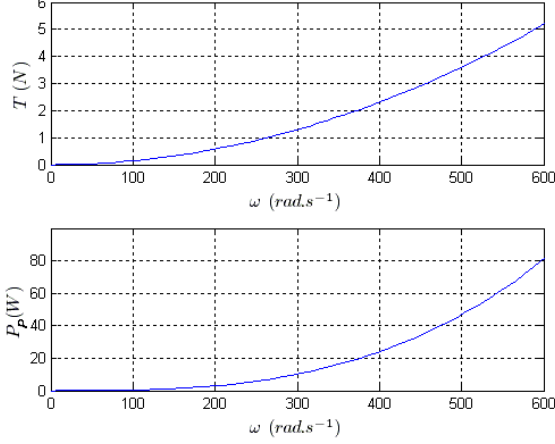


Fig. 3. Theoretical thrust and power of an EPP1045 propeller.

#### IV. QUADROTOR MODELLING

##### A. System dynamics

Writing the equations that portray the complex dynamics of an aircraft implies first defining the system of coordinates to use. Only two reference frames are required, an earth fixed frame and a mobile frame whose dynamic behavior can be described relative to the fixed frame. The earth fixed axis system will be regarded as an inertial reference frame: one in which the first law of Newton is valid. Experience indicates this to be acceptable even for supersonic airplanes but not for hyperonic vehicles [4]. We shall designate this reference frame by  $O_{NED}$  (North-East-Down) because two of its axis ( $u_x$  and  $u_y$ ) are aligned respectively with the North and East direction, and the third axis ( $u_z$ ) is directed down, aligned towards the center of the Earth (Fig. 4). The mobile frame is designated by  $O_{ABC}$ , or Aircraft-Body-Centered, and has its origin coincident with the quadrotor's center of gravity.

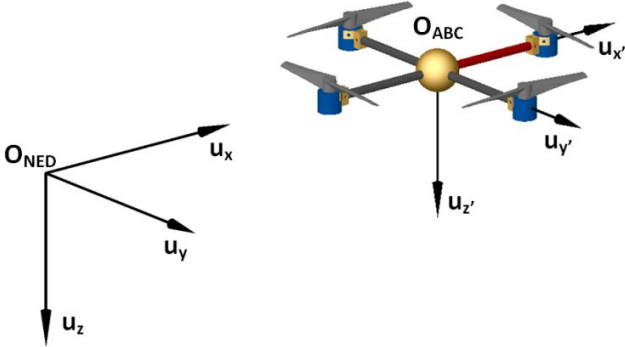


Fig. 4.  $O_{NED}$  and  $O_{ABC}$  reference frames.

In control theory, knowledge about the dynamic behavior of a given system can be acquired through its states. For a quadrotor we assume a state vector  $x$  with 12 states to fully describe its 6 degrees of freedom:

$$x = [U \ V \ W \ P \ Q \ R \ X \ Y \ Z \ \phi \ \theta \ \psi] \quad (5)$$

where we have, from left to right, 3 linear velocities, 3 angular speeds, 3 linear positions and finally the Euler angles (i.e. roll, pitch and yaw), whom are representative of the attitude of an aircraft.

The equations describing the orientation of the mobile frame relative to the fixed one can be achieved by using a rotation matrix. This matrix results of the product between three other matrices ( $R'(\phi)$ ,  $R'(\theta)$  and  $R'(\psi)$ ), each of them representing the rotation of the ABC frame around each one of the  $O_{NED}$  axis [5]:

$$R'(\phi) = \begin{bmatrix} 1 & 0 & 0 \\ 0 & \cos \phi & \sin \phi \\ 0 & -\sin \phi & \cos \phi \end{bmatrix} \quad (6)$$

$$R'(\theta) = \begin{bmatrix} \cos \theta & 0 & -\sin \theta \\ 0 & 1 & 0 \\ \sin \theta & 0 & \cos \theta \end{bmatrix} \quad (7)$$

$$R'(\psi) = \begin{bmatrix} \cos \psi & \sin \psi & 0 \\ -\sin \psi & \cos \psi & 0 \\ 0 & 0 & 1 \end{bmatrix} \quad (8)$$

$$S = R'(\phi)R'(\theta)R'(\psi) \quad (9)$$

where  $S$  is the rotation matrix that expresses the orientation of the coordinate frame  $O_{ABC}$  relative to the reference frame  $O_{NED}$ . To mathematically write the movement of an aircraft we must employ Newton's second law of motion. If we keep the modeling process as simple as possible (i.e. ignoring terms such as Coriolis, Euler and aerodynamic forces) we should arrive at the equation that provides each element of the linear acceleration vector:

$$\begin{bmatrix} \dot{U} \\ \dot{V} \\ \dot{W} \end{bmatrix} = \frac{1}{m} F_p + g \begin{bmatrix} -\sin \theta \\ \cos \theta \sin \phi \\ \cos \theta \cos \phi \end{bmatrix} - \begin{bmatrix} QW - RV \\ RU - PW \\ PV - QU \end{bmatrix} \quad (10)$$

where  $F_p$  is a three element vector with the propeller's force along the three axis of the  $O_{ABC}$  frame and  $g$  is the acceleration of gravity. With application of Newton's second law for rotation we are also able to arrive at the angular accelerations:

$$\begin{bmatrix} \dot{P} \\ \dot{Q} \\ \dot{R} \end{bmatrix} = \begin{bmatrix} \frac{M_x}{I_{11}} \\ \frac{M_y}{I_{22}} \\ \frac{M_z}{I_{33}} \end{bmatrix} - \begin{bmatrix} (I_{33} - I_{22})QR \\ I_{11}RP \\ (I_{22} - I_{11})PQ \\ I_{33} \end{bmatrix} \quad (11)$$

with the elements of the inertial tensor  $I$  equal to:

$$I = \begin{bmatrix} I_{11} & 0 & 0 \\ 0 & I_{22} & 0 \\ 0 & 0 & I_{33} \end{bmatrix} = \begin{bmatrix} 0.0081 & 0 & 0 \\ 0 & 0.0081 & 0 \\ 0 & 0 & 0.0162 \end{bmatrix}. \quad (12)$$

The propellers moments are:

$$M_x = (T_4 - T_2)d_{cg} \quad (13)$$

$$M_y = (T_1 - T_3)d_{cg} \quad (14)$$

$$M_z = (T_1 + T_3 - T_2 - T_4)K_{TM} \quad (15)$$

where  $T_i$  is the thrust of propeller  $i$ ,  $d_{cg}$  is the distance from the motor to the quadrotor's COG (Center Of Gravity) equal to 0.29 m and  $K_{TM}$  is a constant equal to 0.026 m that relates propeller thrust and moment in the following way:

$$K_{TM} = \frac{M}{T}. \quad (16)$$

where the moment vector  $M$  contains the elements of (13), (14) and (15).

### B. Kinematic equations

Here we will study the kinematics of the quadrotor. The first stage of kinematics analysis consists of deriving position to obtain velocity. Let us then consider the position vector  $\vec{r}$ , which indicates the position of the origin of the  $O_{ABC}$  frame relative to  $O_{NED}$ :

$$\vec{r} = X\vec{i} + Y\vec{j} + Z\vec{k}. \quad (17)$$

If we derive each of the components in  $\vec{r}$  we will obtain the instantaneous velocity, which multiplied by matrix  $S$  provides the linear velocities. In this case we can take full advantage of the orthogonality of  $S$  to get:

$$\begin{bmatrix} \dot{X} \\ \dot{Y} \\ \dot{Z} \end{bmatrix} = S^T \begin{bmatrix} U \\ V \\ W \end{bmatrix}. \quad (18)$$

As for rotation we can calculate the Euler rates by using:

$$\begin{bmatrix} \dot{\phi} \\ \dot{\theta} \\ \dot{\psi} \end{bmatrix} = T \begin{bmatrix} P \\ Q \\ R \end{bmatrix} \quad (19)$$

where:

$$T = \begin{bmatrix} 1 & \tan \theta \sin \phi & \tan \theta \cos \phi \\ 0 & \cos \phi & -\sin \phi \\ 0 & \sin \phi / \cos \theta & \cos \phi / \cos \theta \end{bmatrix}. \quad (20)$$

### C. Quaternion differential equations

A problem with the implementation of Euler angles  $\phi$ ,  $\theta$  and  $\psi$  is that for  $\theta = 90^\circ$  the roll angle loses its meaning. In other words, If the aircraft pitches up 90 degrees, the aircraft roll axis becomes parallel to the yaw axis, and there is no axis available to accommodate yaw rotation (one degree of freedom is lost). This phenomenon is designated by gimbal lock. In simulations where complete looping maneuvers may have to be performed that is not acceptable. To overcome this problem, the so called quaternion method may be used. Quaternions are vectors in four-dimensional space that offer a mathematical notation that allows the representation of three dimensional rotations of objects. Quaternions also avoid the problem of gimbal lock and, at the same time, are numerically more efficient and stable when compared with traditional rotation matrices (e.g.  $S$ ) [6]. Therefore, by a quaternion vector  $q$  instead of Euler angles, we can rewrite some kinematic and dynamics equations, such as the time derivative of the rotation quaternion,  $\dot{q}$ :

$$\dot{q} = \frac{1}{2}\Omega_q q + \gamma q = \frac{1}{2} \begin{bmatrix} 0 & -P & -Q & -R \\ P & 0 & R & -Q \\ Q & -R & 0 & -P \\ R & Q & -P & 0 \end{bmatrix} \begin{bmatrix} q_0 \\ q_1 \\ q_2 \\ q_3 \end{bmatrix} + \gamma \begin{bmatrix} q_0 \\ q_1 \\ q_2 \\ q_3 \end{bmatrix} \quad (21)$$

where:

$$\gamma = 1 - (q_0^2 + q_1^2 + q_2^2 + q_3^2). \quad (22)$$

A close look at (2) reveals it is the quaternion equivalent of equation (19). Using the rotation quaternion  $S_q$ :

$$S_q = \begin{bmatrix} q_0^2 + q_1^2 - q_2^2 - q_3^2 & 2(q_1q_2 - q_0q_3) & 2(q_1q_3 - q_0q_2) \\ 2(q_1q_2 - q_0q_3) & q_0^2 - q_1^2 + q_2^2 - q_3^2 & 2(q_2q_3 - q_0q_1) \\ 2(q_1q_3 - q_0q_2) & 2(q_2q_3 - q_0q_1) & q_0^2 - q_1^2 - q_2^2 + q_3^2 \end{bmatrix} \quad (23)$$

we can get the absolute linear velocity:

$$\begin{bmatrix} \dot{X} \\ \dot{Y} \\ \dot{Z} \end{bmatrix} = S_q^T \begin{bmatrix} U \\ V \\ W \end{bmatrix}. \quad (24)$$

And linear accelerations:

$$\begin{bmatrix} \dot{U} \\ \dot{V} \\ \dot{W} \end{bmatrix} = \frac{1}{m} F_p + g \begin{bmatrix} 2(q_1 q_3 - q_0 q_2) \\ 2(q_2 q_3 - q_0 q_1) \\ q_0^2 - q_1^2 - q_2^2 + q_3^2 \end{bmatrix} - \begin{bmatrix} QW - RV \\ RU - PW \\ PV - QU \end{bmatrix} \quad (25)$$

#### D. Modelling of the motor-propeller assembly

The motor-propeller assemblies are essential components of our aircraft since they are responsible for the production of the lifting force that allows flight. This section focuses on modeling the dynamics of these components. As we have seen previously in the quadrotor design section there are many variables to account for when choosing the right motor-propeller assembly. This is mostly because the thrust is a function of several properties such as the propeller's diameter, thrust coefficient and air density. Moreover, although we have 4 "equal" motors, in reality each one of them has a different dynamic behavior. This dissimilarity requires a more precise modelling of the motors, a process that often starts by establishing the relation between the voltage fed to the motor and the matching speed of rotation.

A permanent magnet DC motor transfer function is usually described by a gain and two real poles (also known as a second-order model), respectively associated with mechanical and electrical time constants, being the mechanical constant commonly higher than the electrical one by at least one order of magnitude. In other words, the pole associated with the electrical constant is the faster one and as a consequence the dynamic behavior of such a motor is dominated by the slower pole. Having this knowledge into consideration, a common way to define the dynamic behavior of a DC motor is by using a first order transfer function  $G(s)$ , having only a gain  $K$  and a pole associated with the mechanical time constant  $\tau$ :

$$G(s) = \frac{K}{\tau s + 1} \quad (26)$$

Here arises our first big problem: we know our inputs because we can program the pulse width of the signals that control the speed of the motors, but how can we know our outputs if one does not have direct access to a digital tachometer device? The devised solution for this problem was to build a rudimentary tachometer to get the job done. This device consisted of a simple microphone placed approximately 3 cm away from the tip of the propeller and

high enough not to get hit by it (see Figure 5). The concept behind this technique is quite simple: at each pass of the propeller, air gets pulled downwards of the propeller plane and a microphone's membrane may be able to register the consequent suction effect. Another advantage of using a microphone is the fact that modern day computers can capture sound data of a microphone in real-time, which makes it very useful for any MATLAB® data processing or Simulink® data acquisition that may be required. Following this logic, by using some Simulink® it was possible to provide orders to an Arduino program and capture the sound data of each propeller. Fig. 6 shows a very clear signal form of the propeller sound, where we can clearly identify the sound pressure waves of the passage of the propeller. The motors is revealed to have a nonlinear response, meaning that direct implementation of a first-order transfer function to model the dynamic of each motor is not adequate. To solve this issue it was decided that to obtain a linear model (to allow implementation of first-order transfer functions) the model should be linearized around an adequate operation point. Initial experimental flight tests were executed and revealed that shortly beyond the dead zone the quadrotor took off from the ground. Taking this observation into consideration led to the choice of a relatively low operation point (pulse-width) of 1300 microseconds. Knowing the motors have a time constant of 0.136 seconds, Table I has the gains of the motors transfer functions.



Fig. 5. Microphone positioned to record the propeller sound.

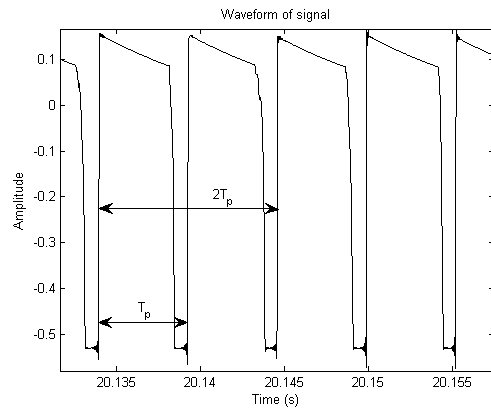


Fig. 6. Propeller sound. Each step in amplitude is a consequence of a propeller blade passage.  $T_p$  is the period between each half-rotation.

#### E. Sensors modeling – Accelerometer

As the name implies, the accelerometer is a sensor that measures accelerations. Typically, accelerometers like the

one installed onboard our quadrotor work through piezo resistive materials, that when deformed by an external force, change the intensity of the electric current flowing through them, providing in this manner a quantification of that force.

Ideally, an accelerometer should be located near the center of gravity of the aircraft. In the case of our quadrotor it is positioned in the coordinates  $(r_x, r_y, r_z)$  indicated in Table II. Given this deviation from the COG, the acceleration vector  $a$  provided by the accelerometer is:

$$a = \frac{1}{m} F_{net} + g \begin{bmatrix} -\sin \theta \\ \cos \theta \sin \phi \\ \cos \theta \cos \phi \end{bmatrix} + \begin{bmatrix} \dot{Q}r_z - \dot{R}r_y \\ \dot{R}r_x - \dot{P}r_z \\ \dot{P}r_y - \dot{Q}r_x \end{bmatrix} + \begin{bmatrix} Q(\text{Pr}_y - \text{Qr}_x) - R(\text{Rr}_x - \text{Pr}_z) \\ R(\text{Qr}_z - \text{Rr}_y) - P(\text{Pr}_y - \text{Qr}_x) \\ P(\text{Rr}_x - \text{Pr}_z) - Q(\text{Qr}_z - \text{Rr}_y) \end{bmatrix} \quad (27)$$

where  $a$  is the sum of all forces acting on the quadrotor. We do not have of gyros onboard the quadrotor. Their absence also makes the determination of the angles of roll and pitch quite tricky because gyros are used for sensor fusion together with accelerometers, providing very steady outputs, thus making them suitable for vibration intensive applications. A rather less robust but direct path to obtain these angles is through the vector of gravitational acceleration provided by the accelerometer, based on the initial approach that we do not intend to move the quadrotor at high speeds (otherwise very high accelerations will indicate roll and pitch angles with very high error):

$$\phi = \arctan \left( \frac{a_y}{a_z} \right) \quad (28)$$

$$\theta = \arctan \left( \frac{a_x}{a_z} \right) \quad (29)$$

where  $a_x$ ,  $a_y$  and  $a_z$  are the vector elements of  $a$ .

#### F. Sensors modeling – Compass

Compasses are scientific instruments used to measure the direction of the magnetic field in the vicinity of the sensor. Among other applications, they are used in aircraft to provide a directional bearing component centered on the north or south poles. The prototype of this thesis uses a compass which serves this exact purpose. Electronic compasses operate using the Hall-effect technology, which is to say that in its interior there are materials which vary the voltage at its terminals when crossed by a magnetic field. Let us assume that the sensor can be modeled as follows:

$$\psi = N_c \quad (30)$$

where  $N_c$  is the direction of the magnetic North Magnetic Pole mapped between  $-\pi$  and  $\pi$  radians.

## V. KALMAN FILTER DESIGN

### A. System linearization

The equations that describe the dynamics of the system are not linear. In such a situation it is common to linearize the equations around an operating point. Linearizing the system will facilitate the construction of the Kalman filter and quadrotor control, as we shall see later.

Let us take as a starting point for the process of linearization the following state vector  $\bar{x}$ , which illustrates nothing less than the quadrotor in flight, stabilized at a height  $z$  from the ground, what is usually known as an equilibrium point (note that the yaw angle, linear position along the y-axis and x-axis can assume any random value, since they do not interfere in the linearization process):

$$\bar{x} = [0 \ 0 \ 0 \ 0 \ 0 \ 0 \ 0 \ 0 \ -1 \ 0 \ 0 \ 0] \quad (31)$$

and also, let us consider the following equilibrium input vector  $\bar{u}$  (i.e. the vector with the speed of rotation of each one of the motors):

$$\bar{u} = [\bar{\omega}_1 \ \bar{\omega}_2 \ \bar{\omega}_3 \ \bar{\omega}_4]. \quad (32)$$

As an example, in the case of the quadrotor,  $\bar{u}$  can be built by finding the angular speed of each motor so that the total thrust produced is equal to the force of gravity. Implementing the first order Taylor series expansion, the linearization of the quadrotor's model (composed by a series of equations that are a function of the states and inputs):

$$\begin{cases} \dot{x} = f(x, u) \\ y = h(x, u) \end{cases} \quad (33)$$

around an operating point  $(\bar{x}, \bar{u})$  is [8]:

$$\begin{cases} \dot{x} = f(x, u) + \frac{\partial f(x, u)}{\partial x} (x - \bar{x}) + \frac{\partial f(x, u)}{\partial u} (u - \bar{u}) \\ y = h(x, u) + \frac{\partial h(x, u)}{\partial x} (x - \bar{x}) + \frac{\partial h(x, u)}{\partial u} (u - \bar{u}) \end{cases} \quad (34)$$

Assuming that the presence of very small disturbances around the equilibrium point  $(\bar{x}, \bar{u})$ ,  $(x - \bar{x})$  and  $(u - \bar{u})$  are both almost zero. In this situation we can verify:

$$\begin{cases} \dot{x} = f(\bar{x}, \bar{u}) = 0 \\ y = h(\bar{x}, \bar{u}) = 0 \end{cases} \quad (35)$$

Therefore, defining:

$$A = \frac{\partial f(x, u)}{\partial x} \quad (36)$$

$$B = \frac{\partial f(x, u)}{\partial u}. \quad (37)$$

$$C = \frac{\partial h(x, u)}{\partial x}. \quad (38)$$

$$D = \frac{\partial h(x, u)}{\partial u}. \quad (39)$$

yields:

$$\begin{cases} \tilde{\dot{x}} = A\tilde{x} + B\tilde{u} \\ \tilde{y} = C\tilde{x} + D\tilde{u} \end{cases} \quad (40)$$

the generic equation for state space representation, with  $\tilde{x} = (x - \bar{x})$  and  $\tilde{u} = (u - \bar{u})$ .

### B. System analysis

If we wish the Kalman filter to be convergent, we must analyze some properties of discrete state space systems such as reachability, controllability and observability.

Starting with the linearized state space form of the quadrotor system:

$$\begin{cases} \dot{x} = Ax + Bu + Gw \\ y = Cx + Du + v \end{cases} \quad (41)$$

where the stochastic variables  $v$  and  $w$  respectively represent the noise affecting the sensor measurements and the aircraft, can be characterized by its respective noise covariances  $R_k$  and  $Q_k$ :

$$Q_k = E\{ww^T\} \quad (42)$$

$$R_k = E\{vv^T\} \quad (43)$$

In practice, the process noise covariances  $Q_k$  and measurement covariances  $R_k$  might change with each time step or measurement, however, here we assume they are constant.

By definition, reachability tells us if it is possible to find a control sequence such that an arbitrary state can be reached from any initial state in finite time. There are several methods for determining if a system is reachable, depending on whether the system matrix  $A$  is or isn't singular (i.e. if  $A$  isn't or is invertible). This property can be investigated by checking the determinant of matrix  $A$ , which in this case equals zero, meaning this matrix is nonsingular. In this case we can immediately say the system is not reachable.

Controllability aims to tell us if it is possible to find a control sequence such that the origin (i.e. when a state equal to zero) can be reached in finite time. For systems in which

matrix  $A$  is nonsingular, we can say the system is controllable if there is a value for  $i$  such that  $A^i$  equals zero. In this case this is true for  $i = 4$ , therefore our system is fully controllable.

Observability refers to the possibility of a given state being determined in finite time using only the system's outputs. This property can be verified if the rank of the observability matrix  $O$ :

$$O = \begin{bmatrix} C \\ CA \\ CA^2 \\ \vdots \\ CA^{N-1} \end{bmatrix} \quad (44)$$

is equal to the system's order  $N$ . The result is 6, meaning we have 6 unobservable states (from the total 12) in the system. This is not surprising as we do not have enough sensors to measure all of the system's states.

In order to produce a suitable Kalman filter we must remove all unobservable and uncontrollable states. This means our system will be reduced to 6 states: the angular velocities and Euler angles.

### C. Filter design

Regardless of the typical connotation of filter as a "black-box" containing electrical networks, the fact is that in most practical applications, the Kalman filter is just a computer program in a central processor. As such, it inherently incorporates discrete-time measurement samples rather than continuous time inputs. Often, the variables of interest, some finite number of quantities to describe the state of the system cannot be measured correctly, and some means of estimating these values from the available data must be generated (i.e. sometimes not all of the states are available). Thus deduction is problematical by the facts that a system driven by inputs other than our own known controls and the relationships among the various state variables and measured outputs are known only with some degree of uncertainty. Furthermore, any measurement will be degraded to some degree by noise, biases, and some device inaccuracies, and so a means of extracting valuable information from a noisy signal must be provided also. There may as well be a number of different measurement devices, each with its own particular dynamics and error characteristics, that supply some information about a particular variable, and it would be desirable to combine their outputs in a methodical and optimal manner. A Kalman filter combines any available measurement data, plus prior knowledge about the system and measuring devices, to generate an estimate of the desired variables in such a manner that the error is minimized statistically (e.g. if we were to run a number of candidate filters many times for the same application, then the average results of the Kalman

filter would be better than the average of any other) [7].

To construct a Kalman filter must we must meet 3 conditions:

1. The model of the system must be linear. Very regularly, even in the presence of nonlinearities, the common approach is to engage in system linearization around an operating point, given that it is easier to work with linear systems;

2. The noise is white, which means it has equal power over all frequencies. This also simplifies the math involved in the filter, for white noise is very similar to the actual noise affecting the system, within limited range of frequencies;

3. The noise has Gaussian density. Typically there are two statistical properties that are easily ascertainable and that characterize a noise signal, the mean and variance, which allows to assume that the noise is Gaussian and simplify the process of filtering from the mathematical point of view.

The optimal solution for the discrete state space Kalman filter is then provided by:

$$\begin{cases} x^k(n) = A^k x(n-1) + B^k \begin{bmatrix} u(n) \\ y(n) \end{bmatrix} \\ y^k(n) = C^k x(n-1) + D^k \begin{bmatrix} u(n) \\ y(n) \end{bmatrix} \end{cases} \quad (45)$$

where  $L$  is the Kalman gain and the matrices of the filter are:

$$A^k = \bar{I} - LC \quad (46)$$

$$B^k = [-LD \quad L] \quad (47)$$

$$C^k = C(\bar{I} - LC) \quad (48)$$

$$D^k = [(\bar{I} - CL)D \quad CM]. \quad (49)$$

where  $\bar{I}$  is the identity matrix. The Kalman gain  $L$  can be calculated through:

$$L = \bar{P}C^T(CPC^T + \bar{R})^{-1}. \quad (50)$$

where  $\bar{P}$  is the steady-state error covariance:

$$\bar{P} = E \left\{ (x - x^k)(x - x^k)^T \right\}. \quad (51)$$

and  $\bar{R}$  is the measurement noise covariance matrix.

## VI. LQR CONTROL DESIGN

In optimal control one endeavors on finding a controller that provides the best possible performance with respect to some given measure of performance (e.g. the controller that uses the least amount of control signal energy to take the output to zero). In this section we try to implement optimum control through the use of a LQR controller (Linear Quadratic Regulator) in which the control signal energy is

measured by a cost function containing weighting factors provided by the controller designer. Moreover, the LQR controller is applicable to MIMO (Multiple-Input Multiple-Output) systems (e.g. in the quadrotor we have the speeds of 4 motors as inputs, and the sensor readings as outputs) for which classical designs are difficult to apply [9].

For a continuous-time linear system described by:

$$\dot{x} = Ax + Bu \quad (52)$$

The cost function  $J_{LQR}$  is [10]:

$$J_{LQR} = \int_0^{\infty} (x^T \hat{Q}x + u^T \hat{R}u) dt \quad (53)$$

where  $\hat{Q}$  (size  $n \times n$ , where  $n$  corresponds to the number of states to control) and  $\hat{R}$  (size  $m \times m$ , with  $m$  the number of process inputs) are both symmetric positive-definite weighting matrices. Consequently, the equivalent discrete-time (discrete because we are going to implement the controller in a digital platform, the Arduino) feedback control law that minimizes the cost value is:

$$u^k = -\bar{K}x \quad (54)$$

where  $u^k$  the vector of control actions and the LQR gain matrix  $\bar{K}$  is provided by:

$$\bar{K} = \hat{R}^{-1}B^T \hat{P} \quad (55)$$

and  $\hat{P}$  is derived by means of the algebraic Riccati equation:

$$A^T \hat{P} + \hat{P}A - \hat{P}B\hat{R}^{-1}B^T \hat{P} + \hat{Q} = 0. \quad (56)$$

A first pick for matrices  $\hat{Q}$  and  $\hat{R}$  is provided by the Bryson's rule which states these matrices as being diagonal:

$$\hat{Q}_k = 1/x_{i,\max}^2 \quad (57)$$

$$\hat{R}_k = 1/u_{i,\max}^2 \quad (58)$$

where  $x_{i,\max}$  and  $u_{i,\max}$  respectively are the maximum tolerable value for each state and input. The core objective of Bryson's rule is therefore to scale the variables in the  $J_{LQR}$  so that the highest tolerable value for each term is one. Particularly, this is very important when  $x$  and  $u$  are numerically very different from each other.

## VII. RESULTS

In this section will observe how the quadrotor system behaves in Simulink<sup>®</sup> and then we will proceed with the LQR controller implementation in the quadrotor prototype.



The Simulink® control loop follows the diagram presented in Figure 7.

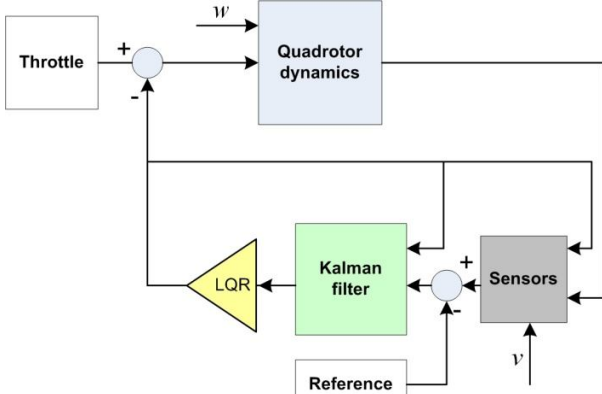


Fig. 7. Quadrotor control loop.

The reference used for the system is:

$$x = [0 \ 0 \ 0 \ 0 \ 0 \ \pi/4] \quad (59)$$

and the quadrotor will start its simulated flight from a position defined by the state vector:

$$x = [0 \ 0 \ 0 \ 0 \ 0 \ 0]. \quad (60)$$

The results are available in Figure 8, in which we can see that the controller can keep the system stable, although there are now wide fluctuations in the pitch and yaw angles. Unfortunately the LQR controller did not work in the real quadrotor prototype. This situation is a consequence of extreme sensor noise (see Fig. 9). This is particularly serious for the accelerometer, whose data is used to estimate the pitch and yaw angles. To try to reduce the noise coming from the sensors, a new Kalman filter was designed with a covariance matrix  $\bar{R}$  calculated from the collected noise data. Consequently, the noise was also introduced in the simulation block of sensors in order to better portray reality. The estimation error proved to be so high that it was impossible to find a functional LQR controller for the system. Even the addition of a low pass filter after the sensors, such as a Butterworth filter, rendered the system impossible to control.

We have seen that we have too much noise for our Kalman filter to handle. It is therefore time to approach the problem from a different perspective in order to achieve a stabilized flight.

We can explore the option of sensor fusion using the current sensor configuration (the tri-axis accelerometer and magnetic compass) together with three angular rate gyroscopes (one for each axis of rotation) to provide more accurate state estimation from noisy measurements. Recalculation of the covariance matrix  $\bar{R}$  (using the new noise data) and implementing it in a new Simulink® model containing three gyroscopes (one of each axis of rotation)

leads to the results in Fig. 10, where we can see that the quadrotor can follow a reference for the yaw angle of  $45^\circ$  while maintaining the attitude of the aircraft stable. This is a consequence of joining the low frequency response of the accelerometer with the high frequency measurements from the gyros yielding accurate estimates for the attitude of the quadrotor.

## VIII. CONCLUSIONS AND FUTURE WORK

We proved that with the current sensor configuration is very hard, if not impossible, to control our quadrotor prototype due to extreme sensor noise. Not even the Kalman filter was able to accurately estimate the states under such conditions. This may be explained by the fact that the system is not reachable. In other words, if the sensor data is corrupted with noise of high intensity, it may be impossible for the Kalman filter to estimate the desired states.

All the work done so far shows only that there are several aspects of the control process that need to be corrected/improved in order to make a controlled flight for this prototype possible. In particular, the inclusion of 3 gyroscopes should be considered, which together with the tri-axis accelerometer, form a combination of sensors that has already been tested in quadrotors, allowing for very good control over its pitch and roll angles. The idea is that with gyroscopes we can determine orientation, but they drift over time (long-term errors), which is something we can correct with accelerometers (short-term errors, i.e. they are very noisy). But even then, we would need something else to correct the drifting yaw angle from the gyroscope, which could be done with a magnetic compass. The long-term idea is that adding a greater number of sensors, in addition to those suggested, can only improve the quality and quantity of states estimated by the Kalman filter. It would also be interesting to develop the simulations further by including new elements such as aerodynamic forces (i.e. wind), collisions and other types of control methods, such as Proportional Derivative controllers.

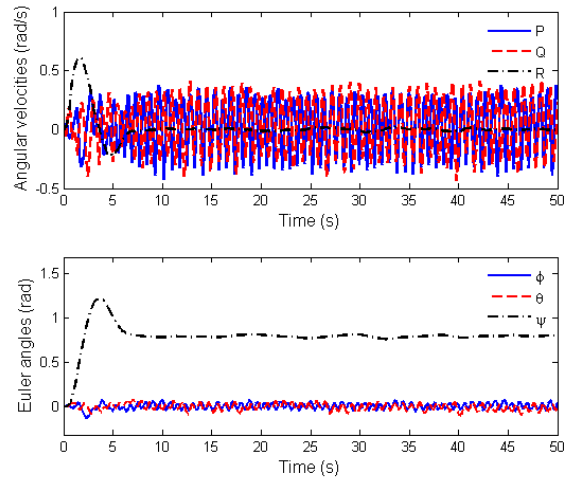


Fig. 8. Time response of the LQR control loop using 6 states, sensors and motors dynamics.

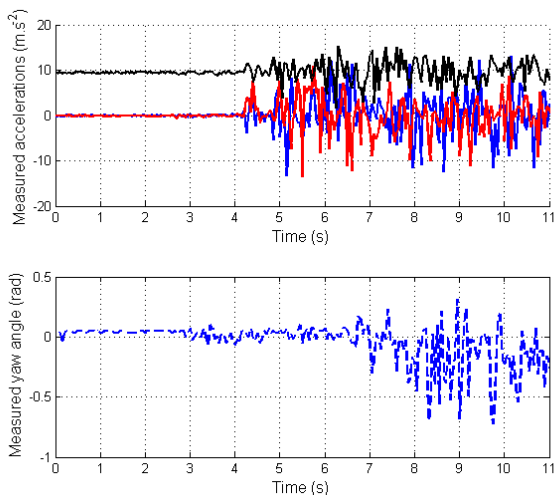


Fig. 9. Sensor noise data (- x-axis acceleration; - y-axis acceleration; - z-axis acceleration; -- compass yaw angle).

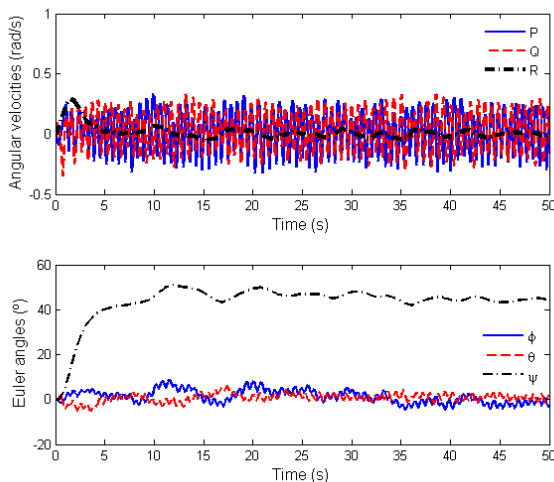


Fig. 10. Time response of the LQR control loop using 6 states and gyros while in the presence of very noisy sensor readings.

The quadrotor prototype should also be taken to an outside environment to see its performance tested under more extreme conditions.

## APPENDIX

TABLE I  
GAINS OF THE TRANSFER FUNCTION DESCRIBING THE MOTORS DYNAMICS

Motor	Gain K
1	2.0276
2	1.8693
3	2.0018
4	1.996

TABLE II  
ACCELEROMETER POSITION RELATIVE TO THE CENTER OF GRAVITY

	Value
$r_x$	0.003 m
$r_y$	0 m
$r_z$	-0.049 m

## ACKNOWLEDGMENTS

First of all, I would like to thank my teachers, Professor José Raul Azinheira and Professor Alexandra Bento Moutinho for their advice, support and availability to speak with me throughout the course of this thesis.

I must not forget thank my colleague Tiago Rita, who shared with me the difficulty of working with a UAV, Tiago Gonçalves also for offering his aid and knowledge on UAVs, and Mr. Raposeiro who helped me with the quadrotor construction.

Last but not least, I want to give special thanks to my family for all their love, support, and for encouraging me to work my way through college, a path that made me gain precious life experiences, which i would have missed otherwise.

## REFERENCES

- [1] <http://en.wikipedia.org/wiki/Quadrotor>, October 2009.
- [2] [http://data.robbe-online.net/robbe\\_pdf/P1101/P1101\\_1-4777.pdf](http://data.robbe-online.net/robbe_pdf/P1101/P1101_1-4777.pdf), February 2009.
- [3] W. Barnes and W. McCormick. *Aerodynamics, Aeronautics and Flight Mechanics*. New York: Wiley, 2nd. edition, 1995.
- [4] J. Roskam. *Airplane flight dynamics and automatic flight controls*. DARcorporation, 2001.
- [5] <http://mathworld.wolfram.com/EulerAngles.html>, May 2009.
- [6] HZ Peter. *Modeling and simulation of aerospace vehicle dynamics*. Virginia: American Institute of Aeronautics and Astronautics, pages 17–242, 2000.
- [7] P.S. Maybeck. *Stochastic Models, Estimation and Control*, Volume 1 Chapter 1, 1979.
- [8] Seth Hutchinson. *Lecture notes on linearization via taylor series*, university of illinois, Spring 2009.
- [9] <http://www.ece.ucsb.edu/roy/classnotes/147c/lqr/qnotes.pdf>, July 2009.
- [10] G.F. Franklin, M.L. Workman, and D. Powell. *Digital control of dynamic systems*. Addison-Wesley Longman Publishing Co., Inc. Boston, MA, USA, 1997.